

Supporting Information for

ORIGINAL ARTICLE

M1-polarized macrophage-derived cellular nanovesicle-coated lipid nanoparticles for enhanced cancer treatment through hybridization of gene therapy and cancer immunotherapy

Ha Eun Shin^a, Jun-Hyeok Han^{a,b}, Seungyong Shin^a, Ga-Hyun Bae^{a,c}, Boram Son^d, Tae-Hyung Kim^e, Hee Ho Park^d, Chun Gwon Park^{b,f,g,*}, Wooram Park^{a,c,g,*}

^a*Department of Integrative Biotechnology, Sungkyunkwan University (SKKU), Suwon, Gyeonggi 16419, Republic of Korea*

^b*Department of Intelligent Precision Healthcare Convergence, SKKU, Suwon, Gyeonggi 16419, Republic of Korea*

^c*Department of MetaBioHealth, SKKU Institute for Convergence, SKKU, Suwon, Gyeonggi 16419, Republic of Korea*

^d*Department of Bioengineering, Hanyang University, Seoul 04763, Republic of Korea*

^e*Department of Integrative Engineering, Chung-Ang University, Seoul 06974, Republic of Korea*

^f*Department of Biomedical Engineering, SKKU, Suwon, Gyeonggi 16419, Republic of Korea*

^g*Korea Institute of Science and Technology (KIST), Seoul 02792, Republic of Korea*

Received 5 January 2024; received in revised form 25 January 2024; accepted 7 February 2024

*Corresponding authors.

E-mail addresses: parkwr@skku.edu (Wooram Park), chunpark@skku.edu (Chun Gwon Park).

Running title: A combined gene-immunotherapy approach against solid tumor

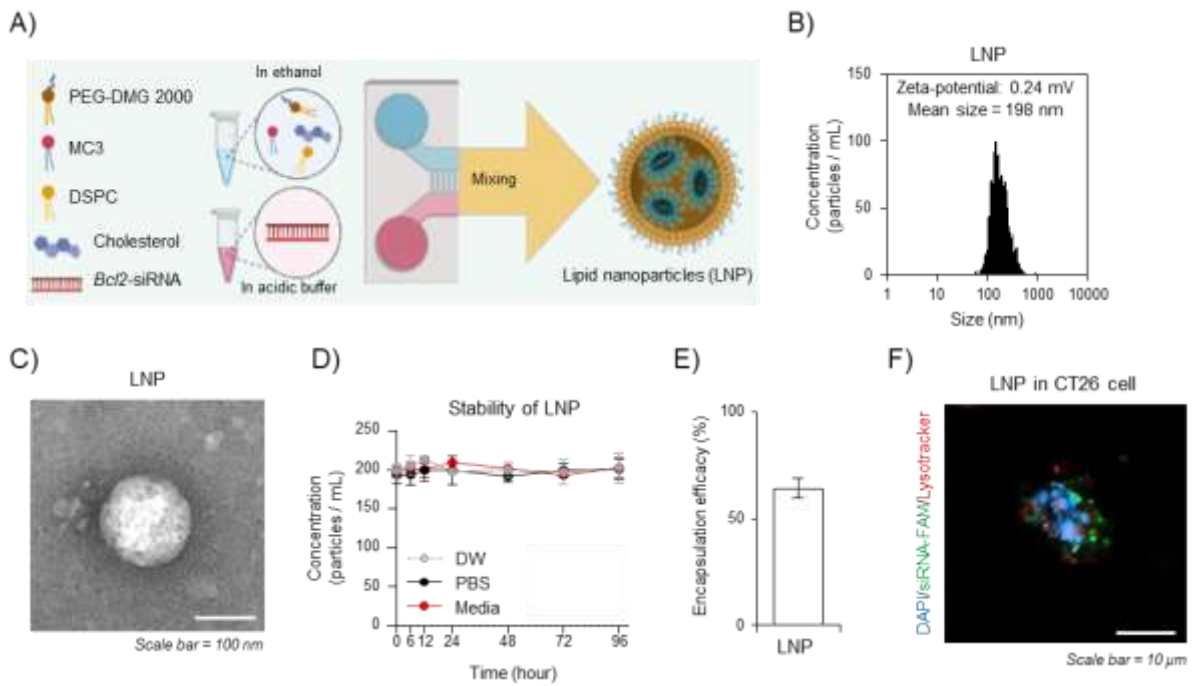


Figure S1 Synthesis and characterization of siRNA-loaded lipid nanoparticles (LNPs). (A) The siRNA-loaded LNPs. (B) Average diameter and surface zeta-potential of LNPs determined by nanoparticle tracking analysis (NTA). (C) Representative transmission electron microscopy image of LNPs. (D) Average diameter for stability of LNPs in deionized water (DW), phosphate-buffered saline (PBS), or cell culture media. (E) Encapsulation efficiency (%) of LNPs with siRNA. (F) Confocal image of CT26 cells after treatment with siRNA-FAM-loaded LNPs. Green, red, and blue colors in the image represent FAM-siRNA, lysosomes, and nuclei, respectively. Scale bar: 10 μm. Data are presented as the mean ± SD (n=3).

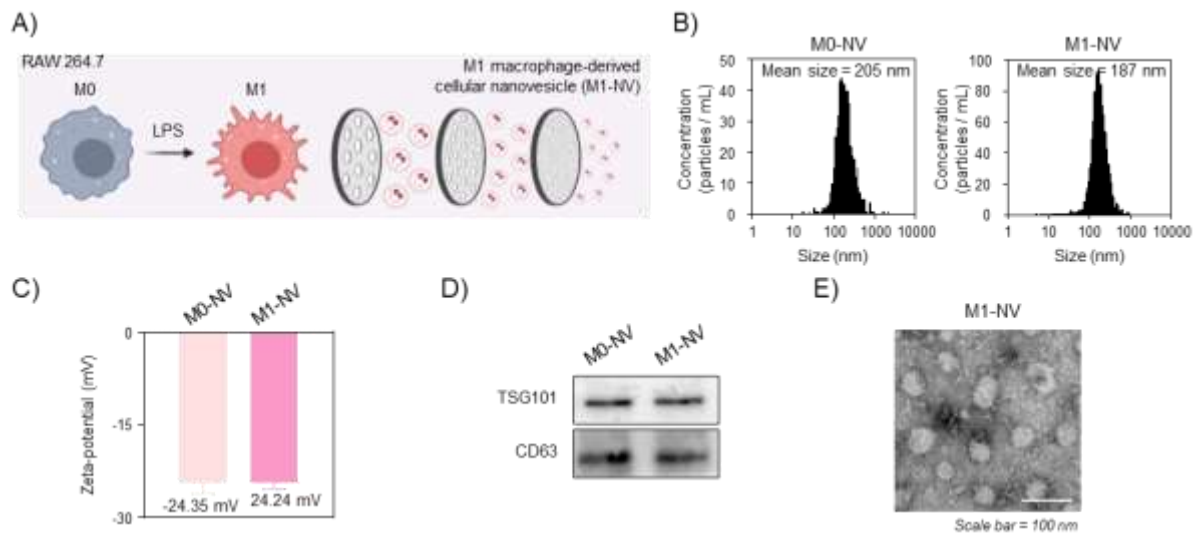


Figure S2 Development of M1 macrophage-derived cellular nanovesicles (M1-NVs). (A) Preparation of M1-NVs. (B and C) Average diameter and surface zeta-potential of M0 macrophage-derived cellular nanovesicles (M0-NVs) and M1-NVs. (D) Expression of exosome markers in M0-NVs and M1-NVs analysed by Western blotting. (E) Representative transmission electron microscopy image of M1-NVs (Scale bar: 100 nm). Data are presented as the mean \pm SD (n=3).

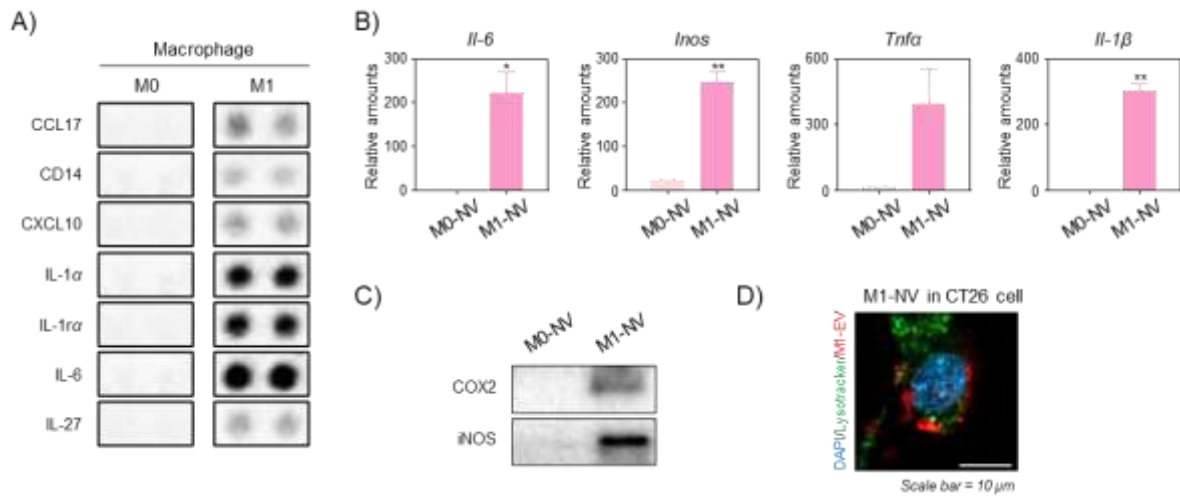


Figure S3 Development and characterization of M1 macrophage-derived cellular nanovesicles (M1-NVs). (A) Analysis of expressed cytokines in M1 macrophages estimated by cytokine array. (B) Expression of RNA levels of inflammatory cytokines in M0-NVs and M1-NVs analysed by real-time PCR. (C) Expression of protein levels of inflammatory cytokines in M0-NVs and M1-NVs estimated by Western blotting. (D) Confocal image of CT26 cells after treatment with M1-NVs. Green, red, and blue colors in the image represent lysosomes, M1-NVs, and nuclei, respectively. Scale bar: 10 μ m. Data are presented as the mean \pm SD (n=3, * P <0.05, ** P <0.01).

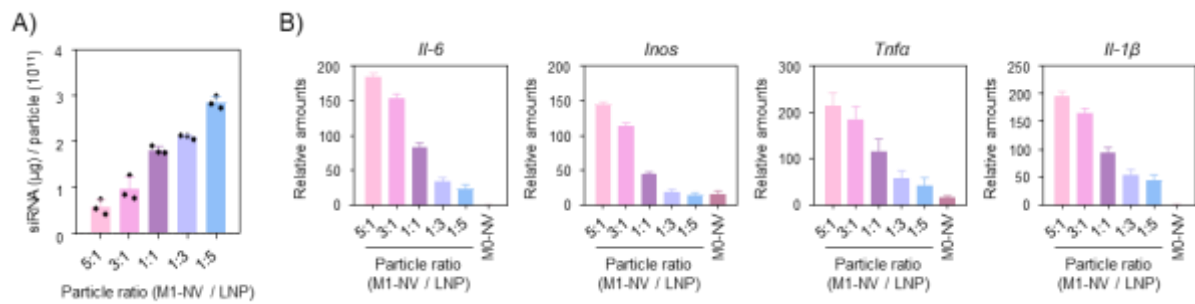


Figure S4 Evaluation of loaded gene and inflammatory cytokines for nanoparticles coated with M1 macrophage-derived cellular nanovesicles (M1-NVs) on lipid nanoparticles (LNPs) at various particle number ratios. (A) Quantitative evaluation of loaded gene in several nanoparticles coated with M1-NVs on LNPs at various particle number ratios using ribogreen assay. (B) Expression of mRNA levels of inflammatory cytokines in several nanoparticles coated with M1-NVs on LNPs at various particle number ratios confirmed by real-time PCR. Data are presented as the mean \pm SD (n=3).

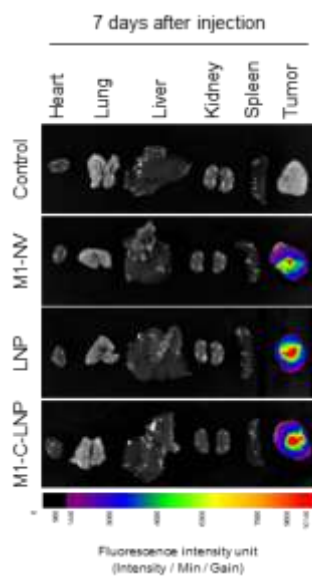


Figure S5 *In vivo* fluorescent image of tissues in CT26 mouse model 7 days after the intratumoral injection of PBS, M1 macrophage-derived cellular nanovesicles (M1-NVs), lipid nanoparticles (LNPs), or M1-NV-coated lipid nanoparticles (M1-C-LNPs).

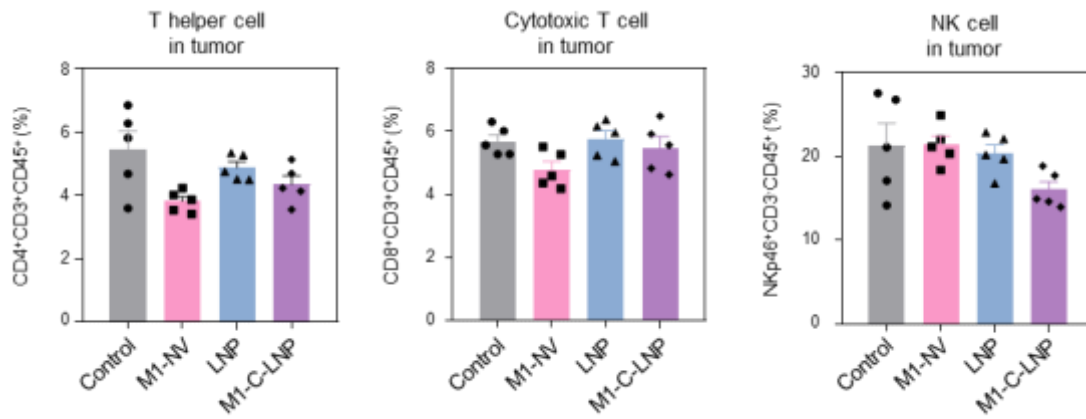


Figure S6 Flow cytometric immunophenotyping of the changed population for intratumoral T and NK cells in CT26 tumor bearing mice model after intratumoral injection of PBS, M1-NVs, LNPs, or M1-C-LNPs. Data are presented as the mean \pm SEM (n=5).

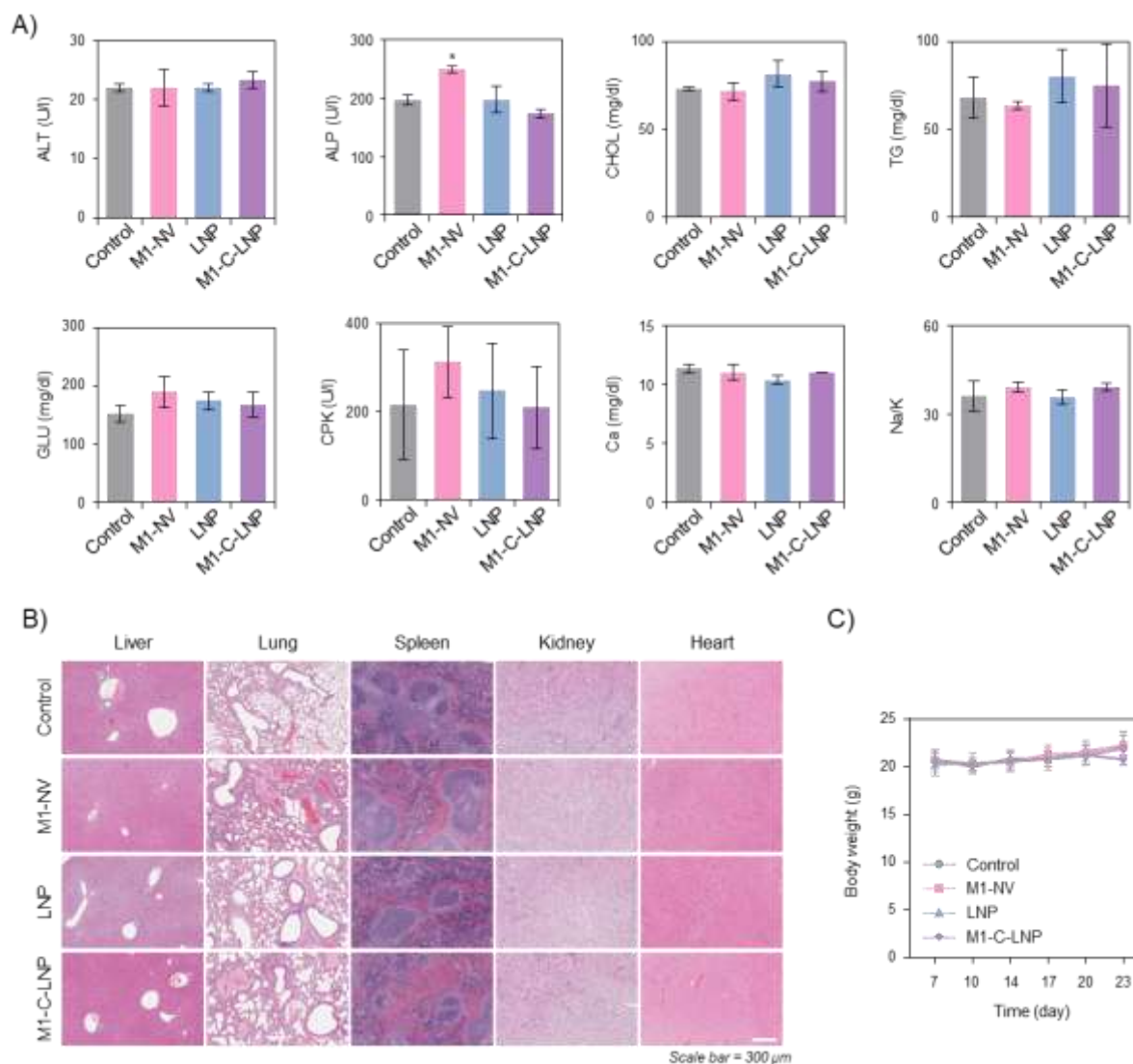


Figure S7 *In vivo* biocompatibility analysis of M1 macrophage-derived cellular nanovesicle-coated lipid nanoparticles (M1-C-LNPs) in CT26 tumor mouse model. (A) Blood biochemical analysis after the administration of PBS, M1 macrophage-derived cellular nanovesicles (M1-NVs), lipid nanoparticles (LNPs), or M1-C-LNPs. (B) Representative images of hematoxylin and eosin (H&E) stained major organs after the administration of PBS, M1-NVs, LNPs, or M1-C-LNPs. Scale bar: 300 μm . (C) Mean change in body weight of mice during treatment with PBS, M1-NVs, LNPs, or M1-C-LNPs. Data are presented as the mean \pm SEM ($n=5$, $*P<0.05$).

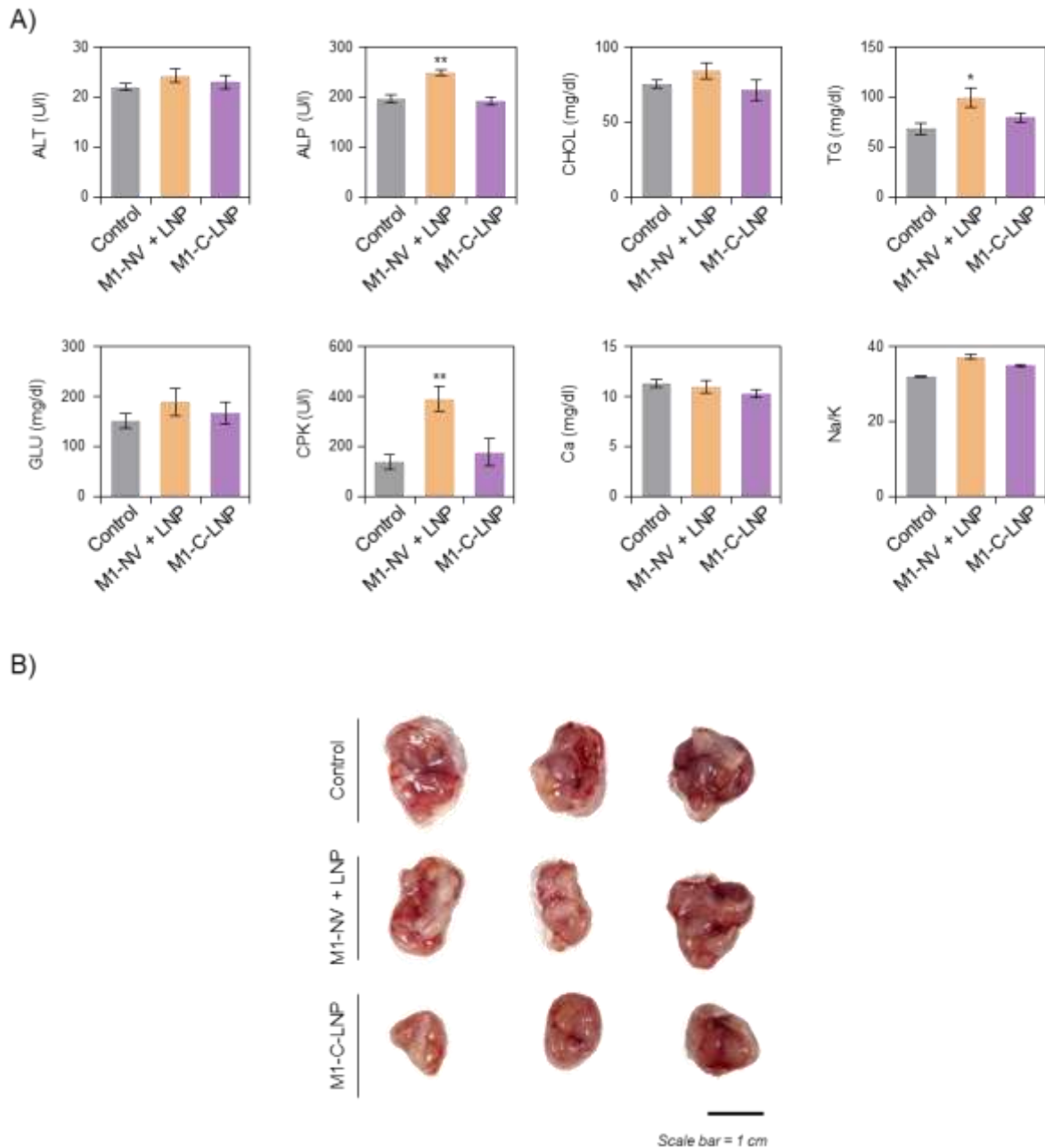


Figure S8 *In vivo* analysis for M1-C-LNPs compared with a simple mixture in CT26 bearing tumor mouse model. (A) Blood biochemical analysis after the administration of the mixture of M1 macrophage-derived cellular nanovesicles (M1-NVs) and lipid nanoparticles (LNPs) or M1-C-LNPs in a CT26 mouse model. (B) Representative images of tumor after the administration of PBS, the mixture of M1-NVs and LNPs, or M1-C-LNPs 7 days after last administration. Scale bar: 1 cm. Data are presented as the mean \pm SEM ($n=3$, * $P<0.05$, ** $P<0.01$).